

Journal of Complex Flow, Vol. 4 No. 1 (2022) p. 1-7

Journal of Complex Flow

Journal homepage: www.fazpublishing.com/jcf

e-ISSN: 2672-7374



Effect of Inner Wall Curvature on Loss Characteristic and Flow Rectification of Curved Diffuser

Muhammad Azfar Muqri Marzuki¹, Normayati Nordin^{1*}, Shamsuri Mohamed Rasidi¹

¹ Centre of Energy and Industrial Environment Studies, Faculty of Mechanical and Manufacturing Engineering, Universiti Tun Hussein Onn Malaysia, Batu Pahat, 86400, MALAYSIA

*Corresponding Author

Received 18 March 2022; Accepted 14 April 2022; Available online 15 May 2022

Abstract: A curve diffuser is frequently used in applications such as HVAC, wind tunnel, gas turbine cycle, aircraft engine, etc., as an adapter to join the conduits of different cross-sectional areas or an ejector to decelerate the flow and raise the static pressure before discharging to the atmosphere. The performance of a curve diffuser is measured according to its pressure recovery and flow uniformity. The paper aims to investigate the effect of inner wall curvature numerically and inflow Reynolds number on loss characteristic, and flow rectification Ansys FLUENT was used to simulate the performance of curved diffuser in terms of static pressure coefficient and flow uniformity index by altering the inner wall curvature ($L_{in}/W_1 = 1.52, 3.99, 8.99, 13.00$ and 25.00) and inflow Reynolds number (Re_{in} = 5.9343 × 10⁴, 8.1628 × 10⁴ and 1.783 × 10⁵). The results show that pressure recovery improved when the inner wall curvature increased from 1.52 to 8.99 for a curved diffuser with an area ratio of 1.6, 2.16, and 4.0. Meanwhile, the increase of inflow Reynolds number caused the flow uniformity to drop at every area ratio of the curved diffuser. The model of the curved diffuser with inner wall curvature of 8.99 and area ratio 4.0 opted as the most optimum producing best pressure recovery up to 0.40 operated at $Re_{in} = 5.9343 \times 10^4$. Meanwhile, the model with inner wall curvature of 25.00 and area ratio 4.0, operated at $Re_{in} = 5.9343 \times 10^4$, was chosen as the best flow performance with an index of 1.92.

Keywords: Inner Wall Curvature, Computational Fluid Dynamics (CFD), ANSYS Fluent

1. Introduction

In applications such as wind tunnel, gas turbine cycle, aircraft engine, and heating, ventilation, and airconditioning (HVAC) systems, diffusers are often introduced as an adapter to connect the ducts of various cross-sectional areas. A diffuser works to reduce the speed of the fluid by increasing the static pressure. Theoretically, a diffuser converts the kinetic energy of the fluid into the pressure energy. It is an ejector to decelerate flow and increase the static pressure before discharging into the atmosphere.

Due to its necessary condition and application, the diffuser can be in various shapes. Two main diffuser types have been used in multiple applications worldwide. A straight diffuser with a zero turning angle is the first type of diffuser. In comparison, the second type is called a turning diffuser or known as a curved diffuser where there can be a range of turning angles. The curved diffuser is mainly used in the wind tunnel and air conditioning duct system to optimize the total length in some instances where the area or spaces are restricted and turn the fluid flow.

The performance of curve diffuser has been actively researched by researchers lately. Two factors are considered that several researchers have determined which is static pressure recovery coefficient and flow uniformity index. Both static pressure recovery and flow uniformity can be increased by altering the design of the diffuser from its geometry and operating parameters like area ratio, angle of turning, turbulent intensity, and Reynold number. Due mainly to the non-uniformity of flow flowing through the curved surface and the complex curved properties of the diffuser, or also known as the curvature effect of the curved diffuser, the primary problem affecting the diffuser output is the creation of flow separation in the convex wall area. The production of secondary flow induced by both the high positive pressure gradient and the adverse pressure gradient inside the curved diffuser is another problem. According to Kumar, flow separation on diffusers needs to be avoided as it can cause pressure loss and affect the pressure recovery [1-3].

In this study, ANSYS computational fluid dynamics (CFD) code FLUENT is used to simulate the performance of curved diffuser in terms of static pressure coefficient and flow uniformity index by altering the inner wall curvature area ratio and Reynold numbers. The optimum inner-wall curvature to produce the maximum performance of the curved diffuser is to be identified.

2. Background Problem

The flow through a curved diffuser is complicated due to the expansion and inflexion introduced along the flow direction. It is found that the flow structure is affected by the area ratio, inlet aspect ratio, centerline length to inlet width ratio, Reynolds number, inlet turbulence intensity and turning angle [4,5]. The generation of secondary flow and flow separation should be avoided as it will cause a decrease in performance. Flow separation in a diffuser needs to be avoided due to the invoked additional pressure loss. The secondary flow is formed by the imbalance between radial pressure gradient and centrifugal forces imposed by circular motion. Due to the complexity, investigation through numerical and experimental on the curved diffuser is challenging. The curvature of the curved diffuser led to the curvature effect. Under a strong adverse pressure gradient, the boundary layer on the inner wall was likely to separate, and the core flow tended to deflect toward the outer wall region [6-9]. Unfortunately, only a little research about the effect of inner wall curvature on the curved diffuser. Therefore, improvement in the background study focusing on how the inner wall curvature affect the performance of the curved diffuser need to be done.

The objectives of this study are to investigate numerically effect of inner-wall curvature on loss characteristics and flow rectification of curved diffuser. Besides that, this research also to propose optimum innerwall curvature for different inflow Reynolds Number and area ratio.

3. Methodology

ANSYS CFD code FLUENT was used to experiment the Pressure Recovery Coefficient, C_p and the Flow Uniformity Index, σ_{out} in inner wall curvature L_{in}/W_l , curved diffuser. The inner wall curvature that was considered were L_{in}/W_l of 1.52, 3.99, 8.99, 13.00 and 25.00 The investigation used a variety of variables, including geometrical and operating parameter. Figure 1 illustrates the overall CFD workflow that involves pre-processing, processing, and post-processing phases.

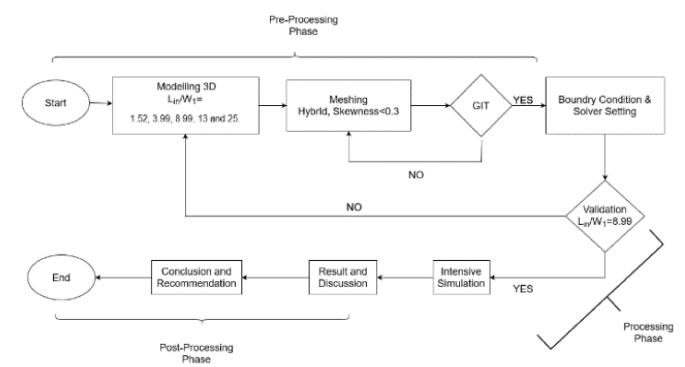


Fig. 1 - Methodology Flowchart

3.1 Modelling and Meshing

Figure 2 shows the curved diffuser for inner wall curvature $L_{\rm in}//W_1$ with turning angle of 90° that was modelled with area ratio of 2.16 to be configure. Near-wall treatments, standard wall function (y+=64) and enhanced wall treatment (y+=1.1 to 1.6) were considered to opt the best could resemble the actual case as shown in Figure 3. Grid independence test was conducted as depicted in Table 2 with Mesh 4 was adopted to provide the least deviation relative to the finest mesh within reasonable CPU solving time [10].



Fig. 2 – Models of Curved Diffuser with inner-wall curvature of 25.00 with area ratio of 2.16

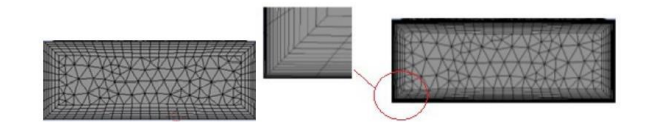


Fig. 3 – Near Wall treatment (a) standard wall function (y+=64) and (b) enhanced wall treatment (y+=1.1 to 1.6)

Table 1 – Grid independent test using

Near wall	Mesh	Element	Nodes	C_p	Dev	
treatment					(%)	
Standard	1	85148	229507	0.53387	0.48	
wall	2	81834	220503	0.53434	0.40	
function	3	81834	220503	0.53434	0.40	
	4	77901	209929	0.53582	0.12	
	5	89297	241644	0.53647	-	
Enhanced	1	379565	379565	0.23651	19.99	
wall	2	394930	394930	0.27581	6.69	
treatment	3	418867	418867	0.27924	5.53	
	4	420214	420214	0.28677	2.98	
	5	431971	431971	0.29559	-	

3.2 Solver and Boundary Condition Setting

The following three-dimensional steady-state Reynolds Averaged Navier Stokes (RANS) equations were numerically solved for a Newtonian, incompressible fluid. The flow was assumed to be fully developed, steady-state and isothermal. The gravitational effect was negligible [11].

Continuity equation,

$$\frac{\partial u}{\partial x} + \frac{\partial v}{\partial y} + \frac{\partial w}{\partial z} = 0 \tag{1}$$

X-momentum equation,

$$u\frac{\partial u}{\partial x} + v\frac{\partial u}{\partial y} + w\frac{\partial u}{\partial z} = -\frac{1}{\rho}\frac{\partial P}{\partial x} + v\left[\frac{\partial^2 u}{\partial x^2} + \frac{\partial^2 u}{\partial y^2} + \frac{\partial^2 u}{\partial z^2}\right] + \frac{1}{\rho}\left[\frac{\partial \left(-\rho u'^2\right)}{\partial x} + \frac{\partial \left(-\rho u'v'\right)}{\partial y} + \frac{\partial \left(-\rho u'w'\right)}{\partial z}\right]$$
(2)

Y-momentum equation,

$$u\frac{\partial v}{\partial x} + v\frac{\partial v}{\partial y} + w\frac{\partial v}{\partial z} = -\frac{1}{\rho}\frac{\partial P}{\partial y} + v\left[\frac{\partial^2 v}{\partial x^2} + \frac{\partial^2 v}{\partial y^2} + \frac{\partial^2 v}{\partial z^2}\right] + \frac{1}{\rho}\left[\frac{\partial(-\rho u'v')}{\partial x} + \frac{\partial(-\rho v'^2)}{\partial y} + \frac{\partial(-\rho v'w')}{\partial z}\right]$$
(3)

Z-momentum equation,

$$u\frac{\partial w}{\partial x} + v\frac{\partial w}{\partial y} + w\frac{\partial w}{\partial z} = -\frac{1}{\rho}\frac{\partial P}{\partial z} + v\left[\frac{\partial^2 w}{\partial x^2} + \frac{\partial^2 w}{\partial y^2} + \frac{\partial^2 w}{\partial z^2}\right] + \frac{1}{\rho}\left[\frac{\partial(-\rho u'w')}{\partial x} + \frac{\partial(-\rho v'w')}{\partial y} + \frac{\partial(-\rho w'^2)}{\partial z}\right]$$
(4)

Table 2 shows, the three types of boundary operating conditions that were imposed. Corresponding to the varied range of inflow Reynolds number $Re_{in} = 5.934 \times 10^4$ – 1.783×10^5 , the inlet velocity V_{in} was 13.255 to 39.829 m/s. At the outlet, the pressure was set at the atmospheric pressure which was 0 gage pressure. At the solid wall, the velocity was zero due to the no-slip condition. Table 3 show the solver setting that was applied. The governing equations were independently solved using a doubleprecision pressure-based solver with a robust pressurevelocity coupling algorithm, SIMPLE been applied. To reduce numerical diffusion, the OUICK scheme was applied for the discretization of the momentum equations, the turbulent kinetic energy equation, and the turbulent dissipation rate equation. A PRESTO discretization scheme was applied for the continuity equation and a default scheme, i.e., Green-Gauss Cell-based, was employed for the solution of the gradient [12,13]. Standard k- ε turbulence model equipped with near-wall treatments, standard and enhanced were considered for the validation. The most optimum solution setting shall provide the least discrepancies with similarity of flow characteristics to the experiment [14,15].

Table 2 - Boundary condition

	Type of boundary	Velocity inlet	
		13.255m/s	
		(5.934×10^4)	
	Velocity magnitude,	18.233m/s	
	V_{in} (m/s)	(8.162×10^4)	
Inlet		39.839m/s	
		(1.783x105)	
		4.1	
	Turbulent intensity, I_{in} (%)	3.9	
		3.7	
	Hydraulic diameter,	70	
	D_h (mm)	72	
Outlet	Pressure	Zero-gauge	
Outlet	Flessule	pressure	
	Working fluids	Air	
Working	Temperature (°C)	30	
fluids	Density, ρ (kg/m3)	1.164	
	viscosity, μ (kg/m.s)	1.872x105	

Table 3 – Solver setting

246200	Sorver seems
Solver Scheme Gradient Pressure Momentum Turbulent Kinetic Energy Turbulent Dissipation Rate	SIMPLE Green-Gaus Cell Based PRESTO QUICK QUICK QUICK
Turbulence Models	standard k-ε (ske) models
Near Wall Treatment	Standard wall function Enhanced wall treatment (EWT)

Pressure Recovery Coefficient (C_p) and flow uniformity index (σ_{out}) are defined as below:

$$C_p = \frac{2(P_{outlet} - P_{inlet})}{\rho V_{inlet}}$$
 (5)

where,

 P_{outlet} = average static pressure at diffuser outlet (Pa) P_{inlet} = average static pressure at diffuser inlet (Pa) ρ = density (kg/m³) V_{inlet} = Inlet velocity (m/s)

$$\sigma_{out} = \sqrt{\frac{1}{N-1}} \sum_{i=1}^{N} (V_{inlet} - V_{out})^2$$
 (6)

where,

N = number of measurement of points V_{inlet} = local inlet air velocity (m/s) V_{outlet} = mean outlet air velocity (m/s)

3.3 Numerical Validation

For validation, turbulence model adopted both standard and enhanced wall treatment was considered. Figure 4 shows that the turbulence model that equipped with enhanced wall treatment had almost resembles result with the experimental case with a deviation percentage of approximately 0.09%.

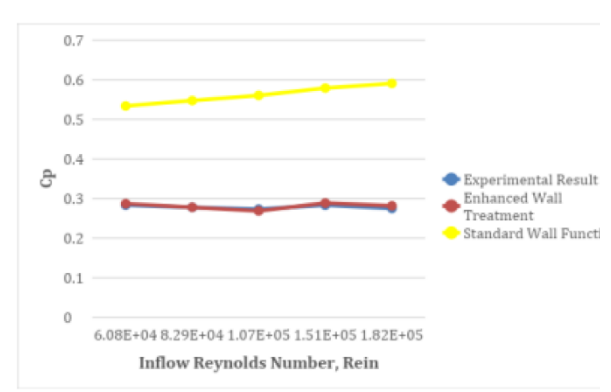


Fig. 4 - Numerical validation

4. Results and Discussion

Effect of inner-wall curvature with different area ratio and inflow Reynolds number on pressure recovery and flow uniformity are evaluated. The most optimum configuration is proposed.

4.1 Effect of Inner Wall Curvature and Reynolds Number on Pressure Recovery

Figure 5 shows the effect of inner-wall curvature L_{in}/W_I on pressure recovery of area ratio 1.6, 2.16 and 4.0 curve diffuser at different Re_{in} . With the increment of inner wall curvature from 1.52 to 3.99 for each area ratio, the pressure recovery also increases. The curved diffuser with area ratio of 4.0 provides the highest recovery of 0.3967. As the inner wall curvature increase to 25, the C_p was reducing. The worst affected was the curved diffuser with area ratio of 1.6 with C_p of -0.159. The result show that applying higher Rein is seen to worsen the performance.

Fundamentally, pressure is recovered when the cross-sectional area increases. However, the vast expansion is always associated with the existence of flow separation, wherein could deteriorate the recovery. From Figure 6, $L_{in}/W_I = 25.00$ relatively forms substantial flow separation within the inner wall region. This undesirable flow phenomenon is not only to disrupt the pressure recovery but more importantly to damage the downstream equipment and generate structural vibration.

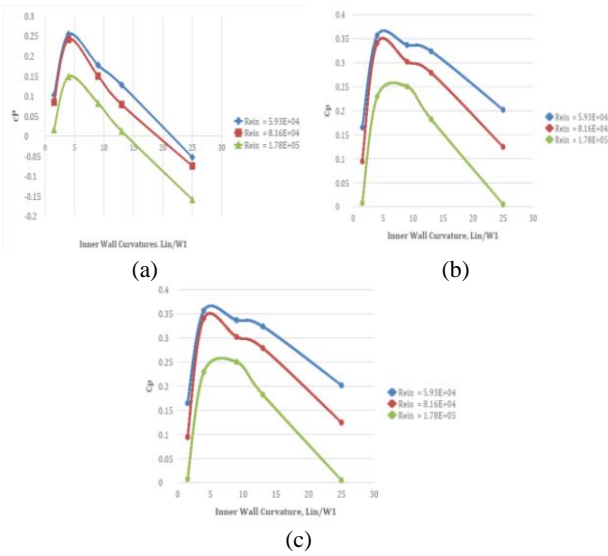


Fig. 5 – Effects of inner-wall curvature on pressure recovery of (a) area ratio 1.6, (b) area ratio 2.16 and (c) area ratio 4.0

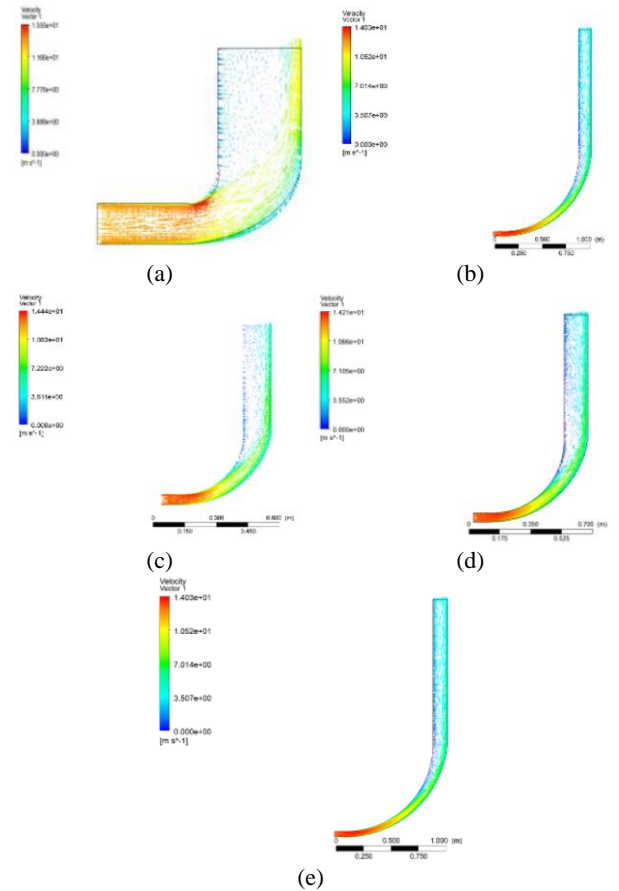
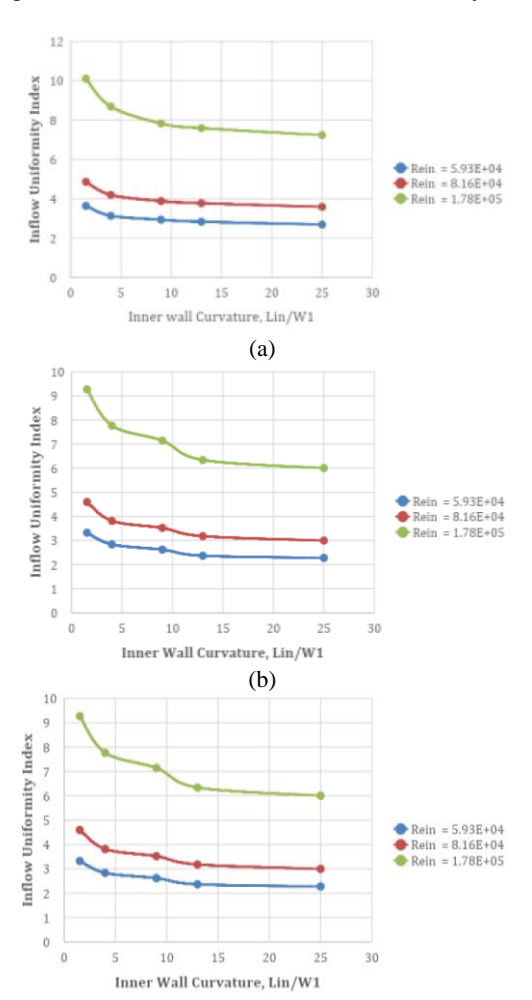


Fig. 6 – Velocity Vector 90° curve diffuser with area ratio 4.0 and inner wall curvature (a) 1.52, (b) 3.99, (c) 8.99, (d) 13.00, and (e) 25.00

4.2 Effect of Inner Wall Curvature and Inflow Reynolds Number on Flow Uniformity

Figure 7 shows the effect of inner-wall curvature on flow uniformity of curved diffuser with area ratio 1.6, 2.16 and 4.0 at different Rein. The flow uniformity more affected by Rein than the inner wall curvature. High Rein can severely distort the flow uniformity. It is worth noted the higher the σ_{out} , the severer the flow uniformity.



(c) Fig. 7 – Effects of inner wall curvature on flow uniformity of area ratio (a) 1.6, (b) 2.16 and (c) 4.0

4.3 Optimum Area Ratio and Inflow Reynolds Number for 90° curved diffuser

Table 5 shows the performance status of 90° curve diffuser with area ratio 1.6, 2.16 and 4.0, inner wall curvature (1.52 to 25.00) and inflow Reynolds number (5.934 x 10^4 to 1.738 x 10^5). In terms of pressure recovery, curve diffuser with inner wall curvature of 8.99 and area ratio of 4.0 is optimal for producing pressure recovery up to 0.40 operated at $Re_{in} = 5.934$ x 10^4 . However, the flow uniformity index obtained is 2.26. in terms of flow uniformity, inner wall curvature 25.00 with area ratio 4.0 operated at $Re_{in} = 5.934$ x 10^4 is the considered configuration due to promising flow uniformity of 1.92. On the other hand, the pressure recovery obtained is 0.32.

There are insignificant differences between these two promising curve diffusers. i.e., inner wall curvature of 8.99 and 25.00 in terms of pressure recovery and flow uniformity. Therefore, upon the need, a compromise between the maximum permissible pressure recovery and flow uniformity can be determined. Whenever the primary concern is the pressure recovery, it is promising to apply inner wall curvature 8.99 and area ratio of 4.0 at *Rein* 5.934 x 104. If the flow uniformity is of interest, it is viable to opt the inner wall curvature 25.00 and area ratio of 4.0 at Rein 5.934 x 10⁴. Figures 8 and 9 illustrate the flow characteristic of both promising configurations. The streamlines in order with no/minimal presence of stalls and vortices.

Table 4 shows, the performances status of 90° curved diffuser.

Table 4 – Performances status of 90° curve diffuser with inner wall curvature 1.52-25.00 and Rein $5.934 \times 10^4 - 1.738 \times 10^5$

		2 10		
Status Performances	Result	Inner Wall	Area Ratio	Rein
		Curvature		
Best pressure recovery (C_p)	0.40	8.99	4.0	5.934 x 10 ⁴
Worst pressure recovery (C_p)	-0.16	25.00	1.6	1.738 x 10 ⁵
Best flow uniformity(σουτ)	1.92	25.00	4.0	5.934 x 10 ⁴
Worst flow uniformity(σουτ)	10.10	1.52	1.6	1.738 x 10 ⁵

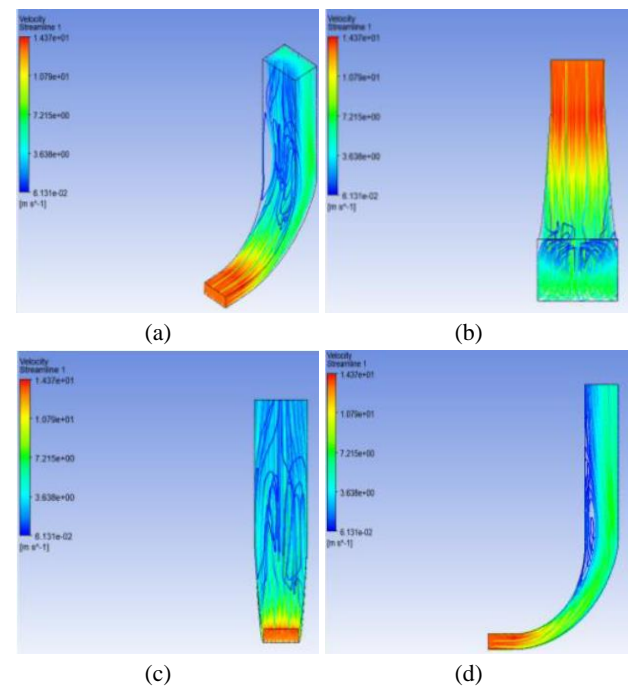


Fig. 8 – 90 $^{\circ}$ curve diffuser with the best pressure recovery (L_{in}/W₁=8.99, AR= 4.0, Re_{in}=5.934 x 104) (a) isometric (b) plan (c) frontal (d) side views

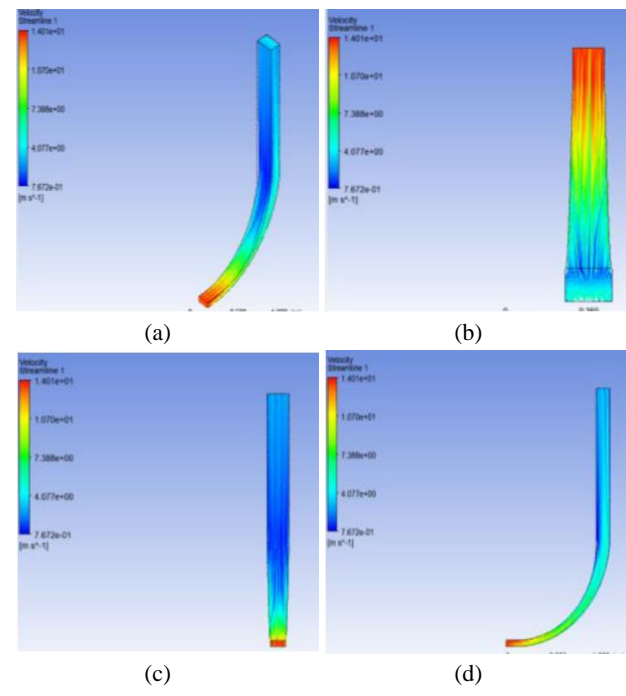


Fig. 9 – 90 $^{\circ}$ curve diffuser with the best flow uniformity (L_{in}/W₁=8.99, AR= 4.0, Re_{in}=5.934 x 104) (a) isometric (b) plan (c) frontal (d) side views

References

- Nordin, N., Abdul Karim, Z.A., Othman, S., and Raghavan, V.R., "The Performance of Turning Diffusers at Various Inlet Conditions." *Applied Mechanic and Materials*. 465-466 (2013): 597–602
- [2] Chong, T. P., Joseph, P. F., and Davies, P. O. A. L., "Parametric Study of Passive Flow Control for a Short, High Area Ratio 90° Curved Diffuser." *Journal of Fluids Engineering*. 130 (11) (2008): 452-456
- [3] Nordin, N., Abdul Karim, Z.A., Othman, S., and Raghavan, V.R., Batcha, M.F.M., Hariri, A., and Basharie, S.M., "Flow characteristics of 3-D turning diffuser using particle image velocimetry." Proceedings of the 7th International Conference on Mechanical and Manufacturing Engineering, 2016.
- [4] Kumaraswamy, R., Natarajan, K. and Anand, R. B. (2019): "CFD Analysis of Flow and Performance Characteristics of a 90° curved Rectangular Diffuser: Effects of Aspect Ratio and Reynolds Number." *International Journal of Turbo & Jet-Engines.* (2019): 583-589
- [5] Saha, K., Singh, S.N., Seshadri, V. and Mukhopadhyay, S., "Computational Analysis on Flow Through Transition s-Diffusers: Effect of Inlet Shape." *Journal of Aircraft*. 44 (1) (2007): 187-193.
- [6] Majumdar, B., Mohan, R., Singh, S. N., and Agrawal, D. P. (1998). "Experimental Study of Flow in a High Aspect Ratio 90 Deg Curved Diffuser." *Journal of Fluids Engineering*. 120(1) (1998) doi:10.1115/1.2819668

5. Conclusion

In conclusion, the effects of inner wall curvature, area ratio and inflow Reynolds number on 90° curve diffuser performances has been successfully investigated with the optimum configuration been proposed. The main findings are highlighted as follows:

- 1. Pressure recovery performance is governed more by the inner wall curvature, while the flow uniformity is by Re_{in} . Optimum L_{in}/W_1 of 25.00 with low $Re_{in} = 5.934 \times 10^4 8.163 \times 10^4$ applied.
- 2. Both *L_{in}/W₁* of 8.99 and 25.00 provide comparable performances, this the selection of a more appropriate model should be based on the needs and restriction.
- 3. L_{in}/W_{I} of 8.99, AR = 4.0, $Re_{in} = 5.934 \times 10^{4}$ is the most optimum configuration to provide the highest-pressure recovery of 0.397 ($\sigma_{out} = 2.26$). Meanwhile the L_{in}/W_{I} , AR = 4.0, $Re_{in} = 5.934 \times 10^{4}$ is the most optimum configuration to provide the flow uniformity at 1.918 ($C_{P} = 0.32$).

Acknowledgement

This research was supported by Ministry of Higher Education through Fundamental Research Grant Scheme (FRGS/1/2018/TK03/UTHM/02/7). We also want to thank to the Universiti Tun Hussein Onn Malaysia (UTHM) for providing facilities to conduct the work.

- [7] Senoo, Y., & Nishi, M. (1977). "Prediction of Flow Separation in a Diffuser by a Boundary Layer Calculation." *Journal of Fluids Engineering*, 99(2) (1977): 379. doi:10.1115/1.3448767
- [8] Hawthorne, W. R., "Secondary Circulation in Fluid Flow." *Proceedings of the Royal Society A: Mathematical, Physical and Engineering Sciences*, 206(1086) (1951), 374–387.doi:10.1098/rspa.1951.0076
- [9] Parsons, D. J., and Hill, P. G. "Effects of Curvature on Two-Dimensional Diffuser Flow." *Journal of Fluids Engineering*, 95(3) (1973): 349. doi:10.1115/1.3447037
- [10] Al-Sammarraie, A.T., and Vafai, K., "Heat Transfer Augmentation through Convergence Angles in a Pipe." *Numer. Heat Transf. Part A Appl.* 72 (2017): 197–214.
- [11] Calautit, J.K., Chaudhry, H.N., Hughes, B.R., and Sim, L.F., "A validated design methodology for a closed-loop subsonic wind tunnel." *Journal of Wind Engineering and Industrial Aerodynamics* 125 (2014): 180–194.
- [12] Nordin, N., Abdul Karim, Z.A., Othman, S., and Raghavan, V.R., "Numerical Investigation of Turning Diffuser Performance by Varying Geometric and Operating Parameters." Applied Mechanic and Materials. 229-231 (2012): 2086–2093.
- [13] Zhang, Q. H., Xu, Y., Shi, W. D., Lu, W. G., & Zhou, L., "Research and Development on the Hydraulic Design System of the Guide Vanes of Multistage Centrifugal Pumps." *Applied Mechanics and Materials*, 197 (2012): 24–30.

- [14] N. Nordin, S. Othman, Raghavan, V.R. and Z.A.A. Karim, "Verification of 3-D stereoscopic PIV operation and procedures", *International Journal Engineering and Technology.* 12(4) (2012): 19-26
- [15] Zhai, Z.J., Zhang, Z., Zhang, W., Chen, Q.Y., "Evaluation of Various Turbulence Models in Predicting Airflow and Turbulence in Enclosed Environments by CFD: Part 1—Summary of Prevalent Turbulence Models." In *HVAC&R Res.* 13 (6) (2007): 853–870.